EPJ Web of Conferences **75**, 03003 (2014)
DOI: 10.1051/epjconf/ 20147503003

Study of the structure influence on the magnetism of $Fe_{70}Al_{30-x}Si_x$ alloys

E. Legarra[1], E. Apiñaniz[2], and F. Plazaola[1]

[1]Dpt. Electricity and Electronics, Basque Country University (UPV/EHU), 48940 Leioa, Spain
[2]Dpt. Applied Physics I, Basque Country University (UPV/EHU), 91944 Vitoria, Spain

Abstract. The influence of the different structures on the evolution of the magnetism in the order-disorder transition produced by mechanical milling in the intermetallic $Fe_{70}Al_{30-x}Si_x$ alloys has been systematically studied by means of XRD measurements, Mössbauer spectroscopy and magnetic measurements. These techniques show that there are two different stages in the evolution of the magnetism during the order-disorder transition and both stages are related to the presence of ordered B2 in annealed alloys. In a first stage the magnetization of the alloys decreases and this decrease corresponds to the presence of B2 structure and the disordering of the $D0_3$ structure. In the second stage the magnetization increases corresponding to the disordering of the B2 structure. Therefore, the increase of the magnetization is related to the disordering of B2 structure, but not to the disordering of $D0_3$ structure. Besides, when plotting the normalized variation of magnetization produced by the disorder versus the normalized variation of lattice parameter we observe a linear relationship, showing that lattice parameter and magnetic properties are also related.

1 Introduction

The mechanical deformation is known to induce disorder in completely ordered Fe-Al alloys. This effect produces a strong influence on the magnetic properties of these alloys. In $Fe_{70}Al_{30}$ alloys a dramatic reinforcement of the magnetism has been observed [1]. This increase of the magnetism has been explained in terms of the change of the local environment [2, 3] where mechanical deformation destroys the intermetallic order in heavily deformed alloys. Furthermore, mechanical deformation causes an increase in volume [4, 5] and the influence of the Fe-Fe interatomic distance on the magnetic moment has been proven both theoretically and experimentally in a few studies [6-8]. Therefore, in order to explain this behaviour the relationship between microstructure and magnetism has to be taken into account, indeed, this is linked to the fact that the Fe-rich side of Fe-Al phase diagram presents three main phases: ordered $D0_3$ and B2, and disordered A2. On the other hand, the Fe-rich side of Fe-Si alloys also show these three phases. However, the magnetic moment decrease with order-disorder transition [9]. For this reason Si is a very appropriate adding element for studying the complex magnetic behavior of $Fe_{70}Al_{30}$ alloys.

The main aim on this work is to study the relationship between the magnetic and structural properties of ball milled $Fe_{70}Al_{30-x}Si_x$ alloys with x=9, 15 and 21 by means of Mössbauer spectroscopy, magnetic measurements and X-ray diffraction.

2 Experimental

The samples have been obtained by means of induction melting in alumina crucibles and cast into ingots under a 40 kPa pressure of high purity argon. Iron, Aluminum and Silicon with a purity of 99.99%, 99.99% and 99.999%, respectively were used. Afterwards, they were powdered by mechanical crushing. The powdered sample was then annealed to obtain large domains of ordered structures ($Fe_{70}Al_{30-x}Si_x$ alloys were annealed at 1223 K/2 h, then cooled down to 823 K and kept there for 1 week). In order to induce disorder the annealed (ordered) alloys were deformed in a planetary ball mill Retsch PM4. The milling process was carried out in air using rotational speeds of 295 r.p.m. during 1, 2, 3, 4, 5 and 10 hours. Chrome steel vials and balls, and ball-to-powder ratio of 10:1 were used.

We have used Co K_α radiation with a Broker-AXS Discover Bragg-Brentano difractometer (CENIM) and the Rietveld method to analyze the X-ray diffractograms (XRD). Magnetic measurements were performed in a VSM magnetometer (Vibrating Sample Magnetometer) at 300 K and 2K from 0 to 10 T and the Mössbauer spectroscopy has been performed by a conventional spectrometer in transmission geometry with a 57Co–Rh source. In order to fit the spectra we have used the NORMOS fitting Program [10].

3 Results and discussion

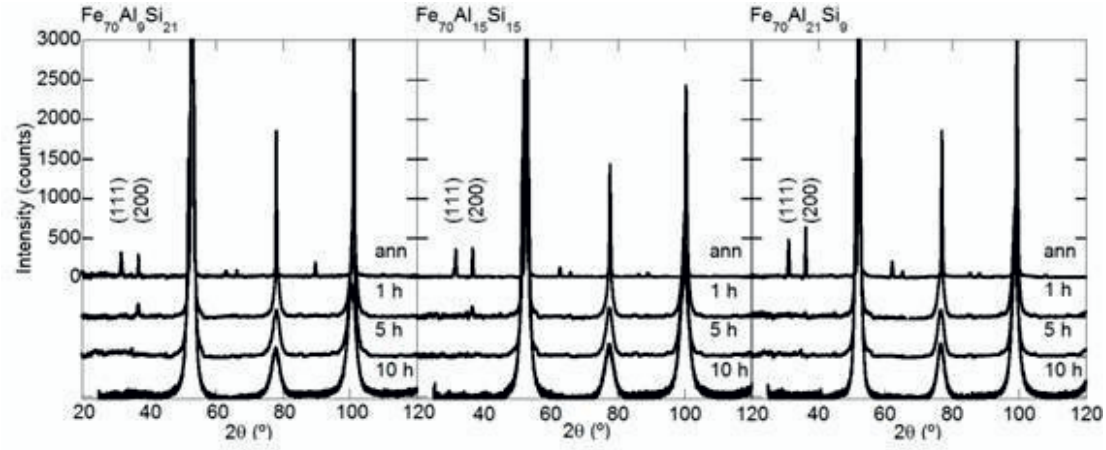

Fig. 1. XRD patterns of annealed and mechanical milled (left) $Fe_{70}Al_9Si_{21}$, (middle) $Fe_{70}Al_{15}Si_{15}$ and (right) $Fe_{70}Al_{21}Si_9$ alloys

The three structures studied in this work ($D0_3$, B2 and A2) have some common peaks. However, the ordered structures ($D0_3$ and B2) have extra peaks in relation to the disordered A2 structure (see figure 1). The appearance of these extra peaks (superstructure peaks) indicates the existence of the ordered structures. In order to distinguish both ordered structures we are going to focus on the (111) and (200) peaks. The presence of the (111) peak is only due to the $D0_3$ structure, whereas the presence of (200) peak is due to both ordered structures.

Figure 1 shows the XRD patterns of the three alloys studied annealed and milled during different hours. XRD patterns of annealed (ordered) alloys present (111) and (200) superstructure peaks. The appearance of both superstructure peaks indicates the existence of $D0_3$ structure. In the 1 hour milled $Fe_{70}Al_{30-x}Si_x$ alloys the (111) superstructure peak characteristic of $D0_3$ structure has disappeared, but the (200) peak common to $D0_3$ and B2 structures is still present. This implies that in $Fe_{70}Al_{30-x}Si_x$ alloys both $D0_3$ and B2 structures are present and that $D0_3$ structure starts to disorder first. The (200) peak disappears with further milling, and after 5 milling hours there is not any superstructure peak (see figure 1).

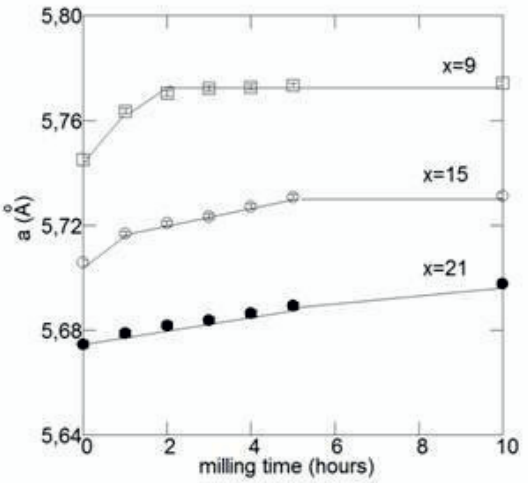

Fig. 2. Lattice parameter versus milling time of $Fe_{70}Al_{30-x}Si_x$

Mechanical deformation causes a progressive lattice parameter increase, in relation to the one of the ordered alloy. This lattice parameter increase reaches a maximum value when disorder has been completely achieved [1]. Therefore, the saturation of lattice parameter can be an indication of complete disorder (A2 structure). Figure 2 shows that the lattice parameter of the alloy with the smallest Si content saturates after 2 milling hours, the lattice parameter of the $Fe_{70}Al_{15}Si_{15}$ alloy saturates after 5 milling hours and for the $Fe_{70}Al_9Si_{21}$ alloy the lattice parameter does not saturate at all in the studied range, and this increase is quite linear with milling time. That is, as Si content increases it is necessary a greater number of milling hours in order to produce the saturation of lattice parameter. Therefore, the addition of Si hinders the disordering process.

Figure 3 shows the evolution of the Mössbauer spectra of $Fe_{70}Al_{30-x}Si_x$ alloys with disordering. The spectra cannot be fitted with discrete subspectra because the alloys present three structures simultaneously ($D0_3$, B2 and A2), which produce a great number of non-equivalent Fe positions. So, these spectra have been fitted by means of hyperfine field distributions. The main inequivalent Fe positions for ordered $D0_3$ and B2 structures with a 70 at.% Fe are 8Fe, 4Fe and 3Fe. The hyperfine field distribution of the annealed alloys shows four main components (around 2T, 12T, 19T and 26T). The values of 26T, 19T and 12T are in agreement with the magnetic hyperfine values of 8Fe, 4Fe and 3Fe position for Fe-Si alloys with a similar Fe content [11]. The component around 2T corresponds to a non-magnetic contribution and cannot be explained in a similar way. The non-magnetic contribution can be caused by the decrease of the number of Fe atoms in the particular surrounding or due to small cluster formation [12]. On the other hand, the spectra corresponding to 10 h of high-energy milling have been fitted with 6 discrete subspectra (one for each Fe position with different number of Fe atoms as nearest neighbours) and the fit is in agreement with samples with disordered A2 structure. We have also fit the 10 milled hour's alloys with hyperfine field distributions in order to compare with the other Mössbauer spectra fits. In these alloys the non-magnetic

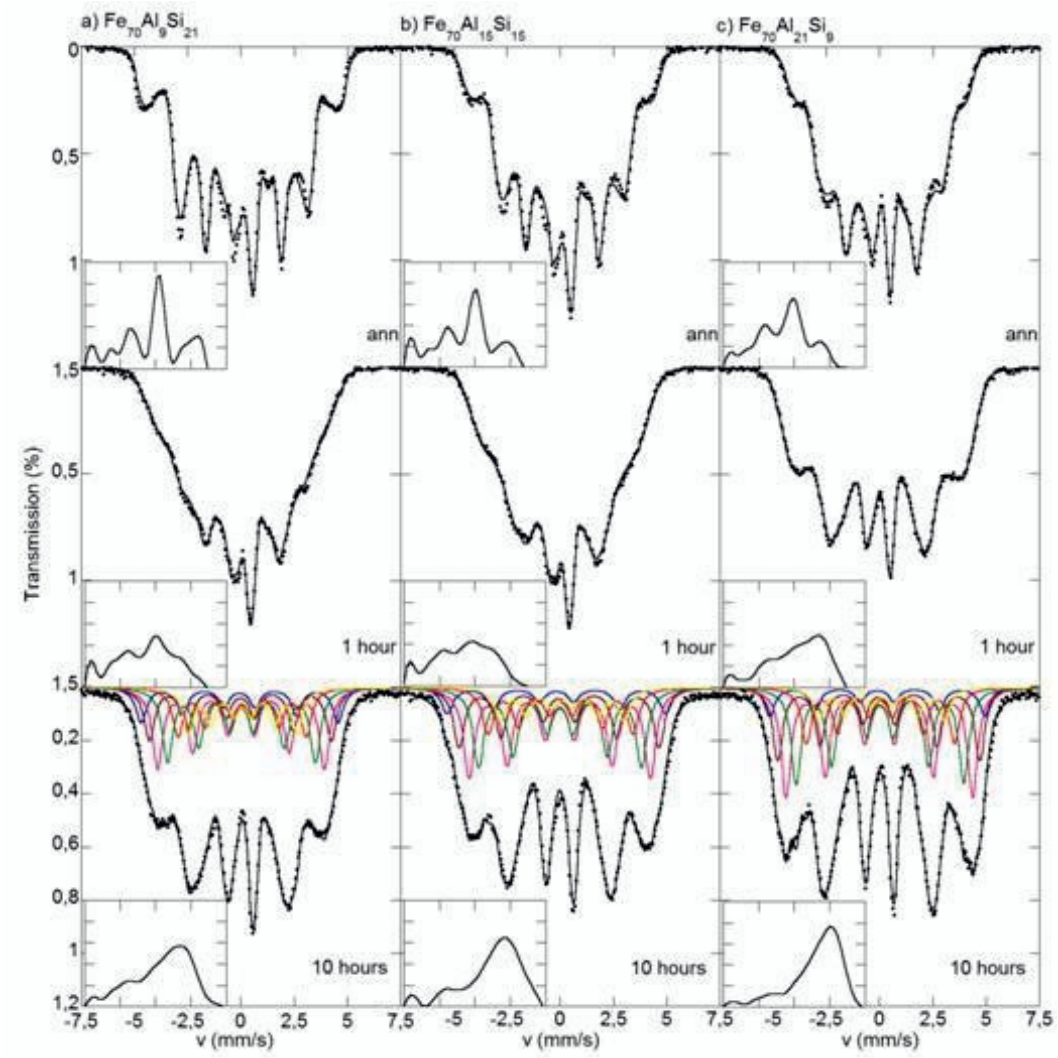

Fig. 3. Fitted Mössbauer spectra of a) $Fe_{70}Al_9Si_{21}$, b) $Fe_{70}Al_{15}Si_{15}$ and c)$Fe_{70}Al_{21}Si_9$ alloys.

component has almost completely disappeared and there is only one main component at high fields (around 26T), in agreement with the fact that the main contributions of A2 structure are present at high fields (7Fe, 6Fe and 5Fe are the most populated surroundings of A2 structure).

Figure 3 also shows the fits of the 1 h milled sample in an intermediate disordering state. The hyperfine field distributions show that the main components observed in annealed alloys have broaden due to a greater number of Fe inequivalent positions produced by the disordering. Furthermore, the area of the component around 19T (4Fe position) decreases in agreement with the fact that $D0_3$ structure has disappeared after 1 milling hour. However, the area of the non-magnetic component of the 1 h milled alloys is similar than the one of the annealed alloys. As XRD pattern have shown that after 1 milling hour the $D0_3$ structure has disappeared but the B2 structure is still present, the non-magnetic component is only related to B2 structure.

In order to analyse in depth the magnetic behaviour of the alloys we have calculated the magnetization at zero field (M_0) of the $Fe_{70}Al_{30-x}Si_x$ alloy series. We have obtained the M_0 value calculating the linear fit of the magnetization measurements at high fields (between 6T and 10T) extrapolated to zero applied field. We have also calculated the slope of this linear fit. Figure 4 shows the evolution of M_0 and the slope of the magnetization curves from 6T to 10T versus the milling time. Figure 4a) shows that M_0 of the alloy with the lowest Si content ($Fe_{70}Al_{21}Si_9$) increases from the first milling hour and M_0 of the other two samples decreases for the first milling hours and then increases. The decrease of the M_0 value coincides with the disappearance of (111) superstructure peak and the presence of the (200) in the XRD patterns (see figure 1). That is, the decrease of the M_0 value is related to the disordering of the $D0_3$ structure and the presence of B2 structure. It is also worth noting that when the M_0 value decreases with milling time the value of the slope increases (see figure 4). All these related facts indicate that the decrease of the M_0 value and the lack of saturation of the magnetization curves are due to the existence of the B2 structure in the samples. And the increase of M_0 starts when the B2 structure has almost disappeared. Therefore, the behaviour of M_0 is related to the B2 structure and not to the increase of A2 structure that was what one could expect. So, the different

behaviours of M_0 of the three alloys are due to the fact that the samples have lost the ordered structures ($D0_3$ and B2) in the alloy with lower Si content ($Fe_{70}Al_{21}Si_9$). That is to say, after 1 milling hour the disorder introduced in the $Fe_{70}Al_{21}Si_9$ alloy with the ball milling is high enough to increase M_0. Figure 4b) also shows that the only alloy that reaches a standard ferromagnetic behaviour (saturation of the M (H) curves, that is, slope zero) is the alloy with the lowest Si content ($Fe_{70}Al_{21}Si_9$) after 10 milling hours. This indicates that the complete disorder (ferromagnetic A2 structure) is achieved only after 10 milling hours.

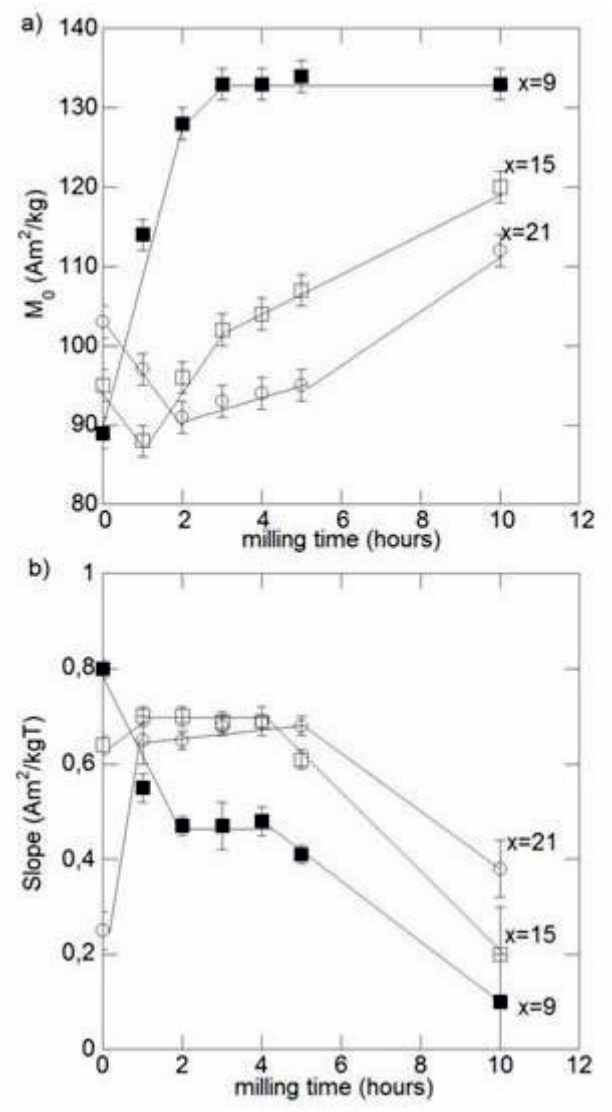

Fig. 4. a) M_0 and b) slope versus milling time of $Fe_{70}Al_{30-x}Si_x$ alloys at RT.

All these data indicate that there are two different stages in the order-disorder transition of $Fe_{70}Al_{30-x}Si_x$ alloys. In the first stage, M_0 decreases and its slope increases, because the $D0_3$ structure is the only structure which is disordering; that is, the B2 structure, related to non-magnetic contributions, is still present. In the second stage, the B2 structure disappears and, therefore, the non-magnetic contribution also disappears. This produces the increase of M_0 and the decrease of the slope, until a standard ferromagnetic behaviour is achieved, indicating that the alloys are completely disordered (only A2 disordered structure).

It is also worth noting that figure 4a) shows that the increase of M_0 between disordered (10 h milled) and ordered (annealed) alloys is lower as Si content increases. This effect cannot be explained in terms of local environment as the three samples have the same structures. On the other hand, the other factor that affects the magnetization in Fe-Al alloys is the increase of lattice parameter [7].

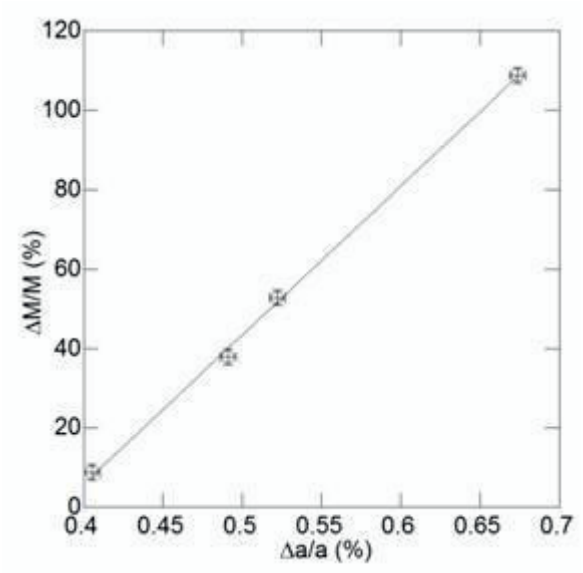

Fig. 5. Normalized variation of M_0 Δ(M/M) versus normalized variation of lattice parameter (Δa/a). The values corresponding to $Fe_{70}Al_{30}$ alloy have been obtained from ref [13].

Figure 5 shows the normalized variation of magnetization versus versus the normalized variation of lattice parameter between disordered (10 h milled) and ordered (annealed) alloys. This figure shows that there is a linear relationship between both parameters. This indicates that the lower increase of M_0 is mainly due to a lower increase of the lattice parameter as Si content increases.

4 Conclusions

The present work shows that as Si content increases the applied mechanical deformation needed to induce a complete order-disorder transition is greater, and the increase of lattice parameter obtained after this transition is lower.

The order-disorder transition has two different stages. In the first stage the magnetization decreases and in the second stage increases. Both stages are related to the presence of ordered B2 structure in the alloys.

The magnetic measurements indicate that the increase of the magnetization decreases with Si content. This decrease is related mainly to the lower increase of the lattice parameter.

Acknowledgements

Financial support from the Spanish CICYT and Basque Government under Grants MAT2012-37923 and IT-443-40 is appreciated.

References

1. E. Apiñaniz, F. Plazaola, J. S. Garitaonandia, D. Martin Rodriguez, J. A. Jimenez, J. Appl. Phys. **93**, 7649 (2003)
2. M. J. Besnus, A. A. Herr, J. P. Meyer, J. Phys. F: Metal. Phys. **5** 2138 (1975)
3. Y. Yang, I. Baker, P. Martin, Phil. Mag. A **79** 449 (1999)
4. X. Amils, J. Nogues, S. Suriñach, M. D. Baro, J. S. Muñoz, IEEE Trans. Magn. **34** 1129 (1998)
5. Hernando, X. Amils, J. Nogues, S. Suriñach, M. D. Baro, M. R. Ibarra, Phys. Rev. B **58** 11864 (1998)
6. E. Apiñaniz, F. Plazaola, J. S. Garitaonandia, J. Magn. Magn. Mater. **272-276** 794 (2004)
7. E. Apiñaniz, F. Plazaola, J. S. Garitaonandia, Eur. Phys. J. B **31** 167 (2003)
8. J. Nogues, E. Apiñaniz, J. Sort, M. Amboage, M d'Astuto, O. Mahon, R. Puznial, I. Fita, J. S. Garitaonandia, S. Suriñach, J. S. Muñoz, F. Plazaola, F. Baudelet, Phys. Rev. B **74** 024407 (2006).
9. W. A. Hines, A. H. Menoti, J. I. Budnick, T. J. Burch, T. Litrenta, V. Niculescu, K. Raj, Phys. Rev. B **13** 4060 (1976)
10. R. A. Brad, J. Lauer, D. M. Herlach, J. Phys. F: Met. Phys. **13** 675 (1983).
11. K. Arzhnikov, L. V. Dobysheva, G. N. Konygin, E. V. Voronica, E. P. Yelsukov, Phys. Rev. B **65** 024419
12. J. L. Dormann, D. Fioran, E. Tronc, Adv. Chem. Phys. **98** 283 (1997)
13. E. Apiñaniz, J. S. Garitaonandia, F. Plazaola, D. Martin Rodriguez, J. A. Jimenez, Sens Act A **106** 76 (2003)